XFires
D1.2 ECV Inventory Document (EID)

Project Name	Climate-Space – Theme II: Cross-ECV activities: XFires
Contract №	4000145351/24/I-LR
Issue Date	13/03/2025
Version	1.1
Author	M. Lucrecia Pettinari
Document Ref.	XFires_D1.2_EID_v1.1
Document type	Public

To be cited as: Pettinari M.L. (2025) ESA CCI XFires: D1.2 ECV Inventory Document (EID), version 1.1.
Available at: https://climate.esa.int/en/Cross_ECV_Projects/xfires/key-documents

Project Partners

Prime Contractor	UNEXE – University of Exeter (United Kingdom)
CORE Partners	UNEXE – University of Exeter (United Kingdom) UAH – University of Alcala (Spain) LSCE-UVSQ – Laboratoire des Sciences du Climat et de l'Environnement, Université de Versailles St Quentin en Yvelines (France) WUR – Wageningen University (Netherlands)
ECV Partners	UCLou – Université Catholique de Louvain (Belgium) UoL – University of Leicester (United Kingdom) TUWien – Technische Universitaet Wien (Austria) BIRA-IASB – Royal Belgian Institute for Space Aeronomy (Belgium) CNR-IREA – National Research Council of Italy – Institute for Electromagnetic Sensing of the Environment (Italy) DTU – Technical University of Denmark (Denmark)

Distribution

Affiliation	Name		Copies
ESA	Clément Albergel (ESA)		electronic copy
Project Team	Stephen Sitch (UNEXE) James M. Haywood (UNEXE) Emilio Chuvieco (UAH) M. Lucrecia Pettinari (UAH) Carlota Segura-García (UAH) Erika Solano (UAH) Patricia Oliva (UAH) Philippe Ciais (LSCE-UVSQ) Simon Bowring (LSCE-UVSQ) Yidi Xu (LSCE-UVSQ)	Guido van der Werf (WUR) Roland Vernooij (WUR) Pierre Defourny (UCLouvain) Céline Lamarche (UCLouvain) Darren Ghent (UoL) Wouter Dorigo (TU Wien) Daan Hubert (BIRA-IASB) Daniela Stroppiana (CNR-IREA) Monica Pinardi (CNR-IREA) Louise Sanderberg Sørensen(DTU)	electronic copy

Summary

This Essential Climate Variables (ECV) Inventory Document (EID) lists and summarizes the relevant datasets (both ESA ECVs and other data) that will be needed to perform the analyses of extreme fires.

	Affiliation/Function	Name	Date
Prepared	UAH	M. Lucrecia Pettinari	03/03/2025
Reviewed and Approved	UNEXE - Science Leader	Stephen Sitch	03/03/2025
Accepted	ESA - Technical Officer	Clément Albergel	14/03/2025

Document Status Sheet

Issue	Date	Details
1.0	03/03/2025	First version of the document
1.1	13/03/2025	Addressing comments from ESA's Technical Officer

Document Change Record

#	Date	Request	Location	Details
1.0	03/03/2025	UAH	All document	First release of the document
1.1	13/03/2025	ESA	Section 4	New section added

Table of Contents

List of Figures

1. Burned Area Datasets

Since the objective of the XFires project is to analyse the occurrence, characteristics and impacts of extreme fires, the main ECV to be used in the project is Fire Disturbance, and more specifically, burned area. The dataset to be used is FireCCI51, since it has the longest time series of the medium-resolution products generated within the project.

1.1. FireCCI51

The FireCCI51 burned area (BA) product was developed as part of the ESA CCI ECV Fire Disturbance project. The main input for the FireCCI51 algorithm are the MOD09GQ Collection 6 images, acquired by the Terra satellite, which offer daily surface reflectance information in the RED and near infrared (NIR) bands of the MODIS sensor at 250 m spatial resolution. Complementary to the surface reflectance product, the daily MOD09GA Collection 6 product was also used to extract information on the quality of the data (quality flags), as well as the MCD14ML Collection 6 product (that uses Terra and Aqua MODIS data) to extract thermal information (Giglio et al., 2016). Land cover information from the Land Cover CCI project has also been used. The description of the algorithm can be found in the Algorithm Theoretical Basis Document (Lizundia-Loiola et al., 2018) and in Lizundia-Loiola et al. (2020).

This BA product is published in two formats: pixel and grid product. For the XFires project, the grid product is used, while the pixel product is not used directly, but as its derived fire patches dataset FRY2.0 (see Section 0). The grid product is the result of summing up the area of the pixels classified as burned from the pixel product within each cell of 0.25 degrees in a regular grid covering the whole Earth in monthly composites provided as NetCDF files. In addition to this variable, other attributes are stored in the NetCDF file: standard error of the estimations, fraction of burnable area, fraction of observed area, and the burned area for 18 land cover classes of the Land Cover CCI (LC_cci product, ESA (2017)). Figure 1 shows an example of the FireCCI51 grid product, accumulated for the year 2019.

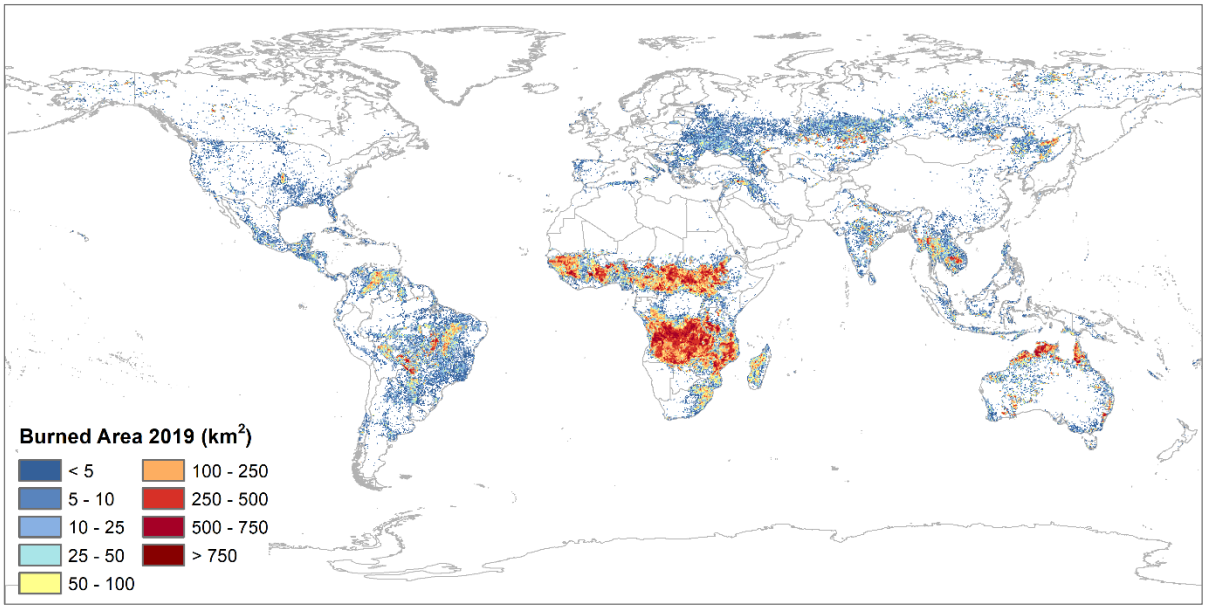

Figure 1: FireCCI51 grid product corresponding to the total BA for the year 2019.

1.2. FRY2.0

The FRY dataset is a global fire patch functional traits dataset, based on the FireCCI51 pixel product (Chen et al. in revision). This dataset, in its version 2.0, creates polygons of burned patches using the burned date (date of first detection layer of FireCCI51) as the basic component where all pixels are spatially connected with a queen neighbourhood and are adjacent to at least another burned pixel with an absolute difference in date below a fixed cut-off value (in days). The detailed procedure for the creation of the polygons is explained in Chen et al. (in revision). Figure 2 shows the FRY2.0 corresponding to the year 2017.

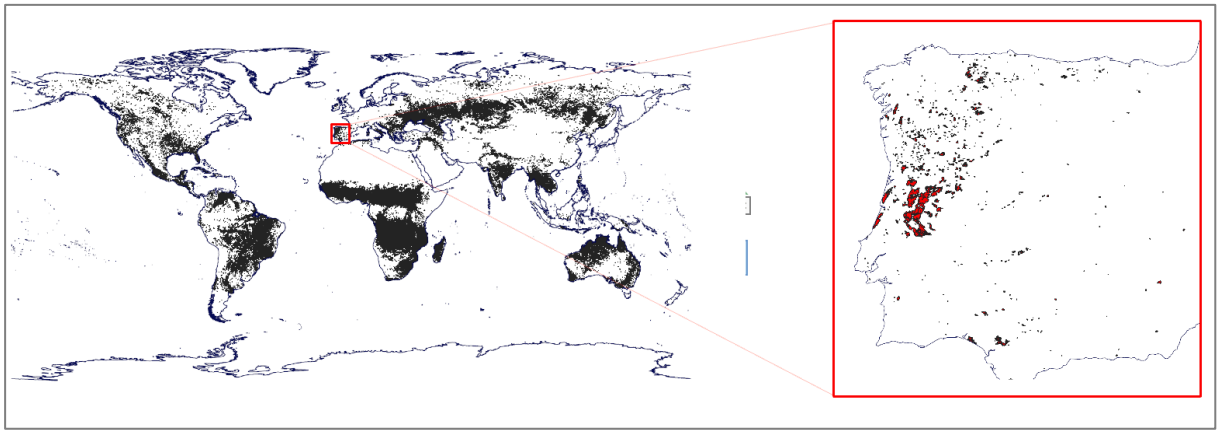

Figure 2: Global map of the fire shapefiles for the year 2017 generated from FireCCI51, with a screen shot over the Iberian Peninsula.

The fire patches are provided as ESRI Shapefiles, and include several variables related to fire patch morphology and functional traits, and ancillary information obtained from external sources. The ones being used for the analysis of extreme fires are:

- **Fire Size**, calculated as the sum of area of each pixel inside a fire patch.
- **Minimum and maximum burn date**, corresponding to the date of the first and last detected burned pixel of the fire patch, which allows to obtain the **fire duration** of each fire patch.
- **Rate of Spread (ROS)**, calculated as the longer axis of a fire patch's standard deviation ellipse divided by the fire duration in days.
- **Fire Radiative Power (FRP)** data from the MODIS Collection 6 thermal anomalies (MCD14ML, Giglio et al., 2016) dataset were projected over each fire patch, for which the median, minimum, maximum FRP during 30 days after ignition was computed (Laurent et al., 2019).
- **Fire Severity** based on the MOdis burn SEVerity global database MOSEV derived from the MODIS 500m resolution differential Normalized Burn Ratio (Alonso-Gonzalez and Fernandez-Garcia 2021).

2. Other ESA ECVs

2.1. CCI Biomass

The CCI BIOMASS project delivers spatially explicit estimates of above ground biomass (AGB) for three epochs and their related standard deviations as separate map products (Santoro et al. 2024). The AGB product consists of global datasets with estimates of AGB (where the unit of Mg ha-1 = tons ha-1). AGB is defined as the mass, expressed as oven-dry weight, of the woody parts (stem, bark, branches and twigs), of all living trees excluding stump and roots.

The maps currently available cover 2010, and yearly for the period 2015 to 2021. They are provided at full spatial resolution (100 m), and at a coarser resolution of, between others, 25 km (which they consider to be 0.25 degrees). Figure 3 shows the global AGB estimates for the year 2020.

This dataset will be used as an input to the machine learning (ML) fire model and the biomass recovery model.

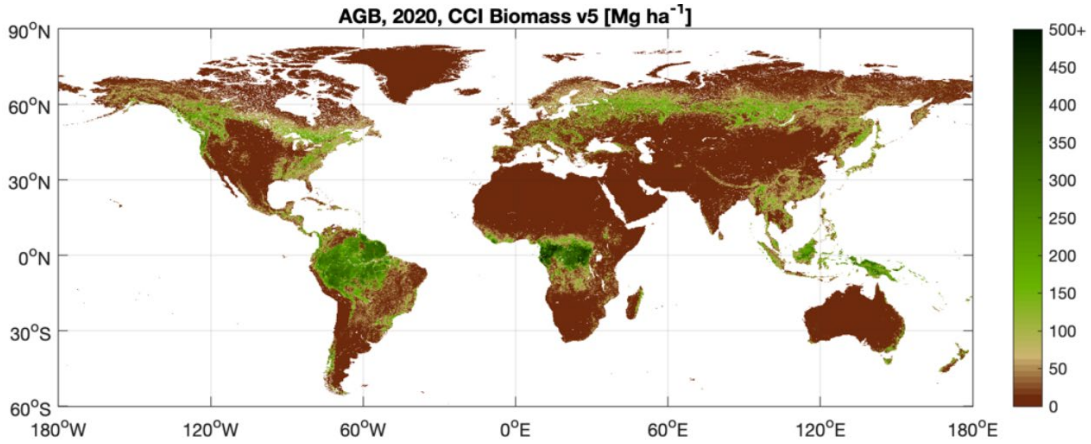

Figure 3: Global AGB estimates for the year 2020 with a 100-m spatial resolution (extracted from Santoro et al. 2024).

2.2. CCI Land Cover

The Land Cover algorithm developed within the CCI programme generated maps from 1992 to 2015, and that algorithm was then transferred to the Copernicus Climate Change Service (C3S), where the production continued for the period 2016 to 2022 (Defourny et al. 2024). The products are based on Proba-V, Sentinel-3 OLCI and Sentinel-3 SLSTR data, at a spatial resolution of 0.002778 degrees (approx. 300 m at the Equator). The datasets from both sources (CCI and C3S) are spatially and temporally consistent. The typology was defined using the Land Cover Classification System (LCCS), consisting of 23 classes, 18 of which include vegetation and can be considered burnable.

Figure 4 shows the land cover map corresponding to 2022. This dataset will be used as an input for the ML and process based fire models.

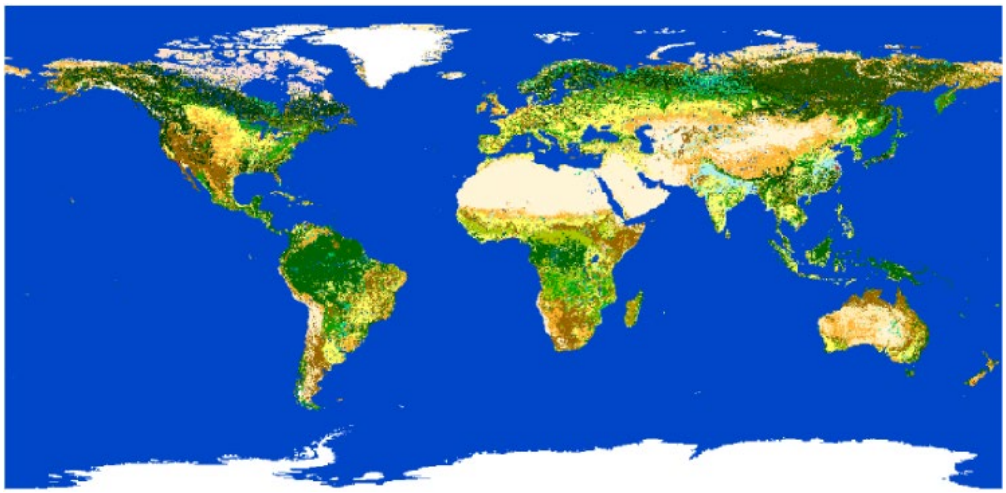

Figure 4: Most recent land cover map from the time series, corresponding to 2022, at 300 m spatial resolution (Defourny et al. 2024).

2.3. CCI Land Surface Temperature

The Land Surface Temperature (LST) ECV is comprised by a suite of datasets based on multiple sensors. They are provided in different spatial resolutions, from 0.1 to 0.25 degrees, and with temporal resolutions from 1 hour to daily and monthly (Ghent et al. 2021). The time span of the products depends on the input sensor, and in the case of datasets based on multiple sensors, they span from 1995 to 2020.

Figure 5 shows an example of one of the products for 15 September 2011. For further details of each of the available datasets, refer to Ghent et al. (2021, 2023). These datasets will be used as model inputs for ML and process based fire models.

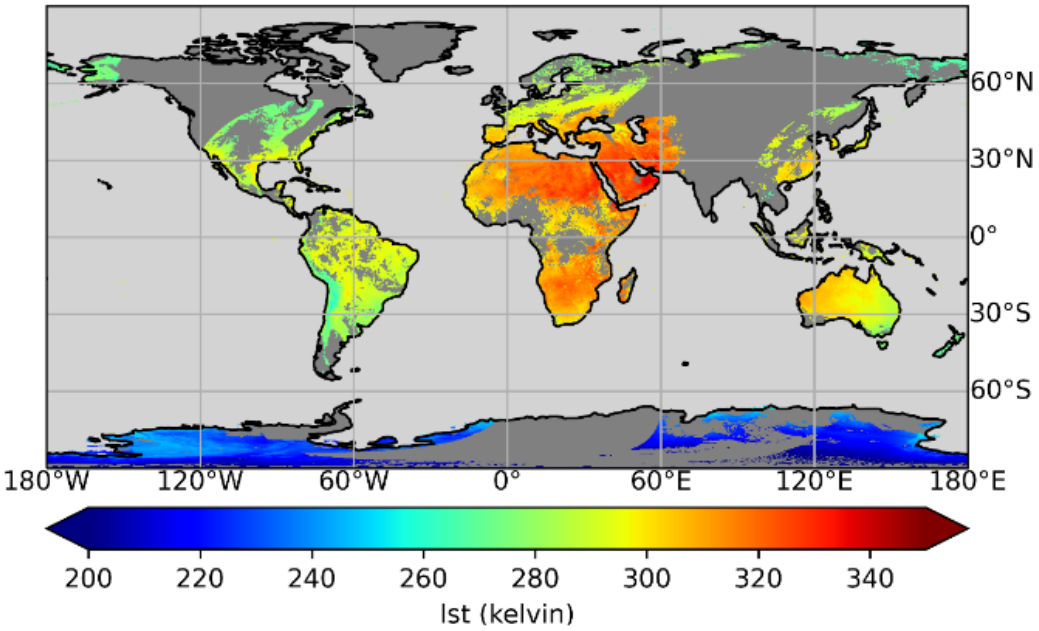

Figure 5: Example of MULTISENSOR_IRMGP_L3S_0.05 daily daytime data for 09:00 UTC on 15 September 2011, extracted from Ghent et al. (2021).

2.4. CCI Soil Moisture

The CCI Soil Moisture (SM), in its current version v08.1 consists of three surface SM data sets: the “ACTIVE Product” and the “PASSIVE Product” were created by fusing scatterometer and radiometer soil moisture products, respectively, while the “COMBINED Product” is a blended product based on the former two data sets. Data files are provided as NetCDF-4 classic format and comprise global merged surface soil moisture datasets at daily temporal resolution. The data set spans over 40 years covering the period from November 1978 to December 2022 (van der Schalie et al. 2023). The SM products provide surface SM with a global coverage and a spatial resolution of 0.25°, and a temporal resolution of 1 day.

Figure 6 shows the mean SM anomaly for 2022. This dataset will be used as model inputs for ML and process based fire models.

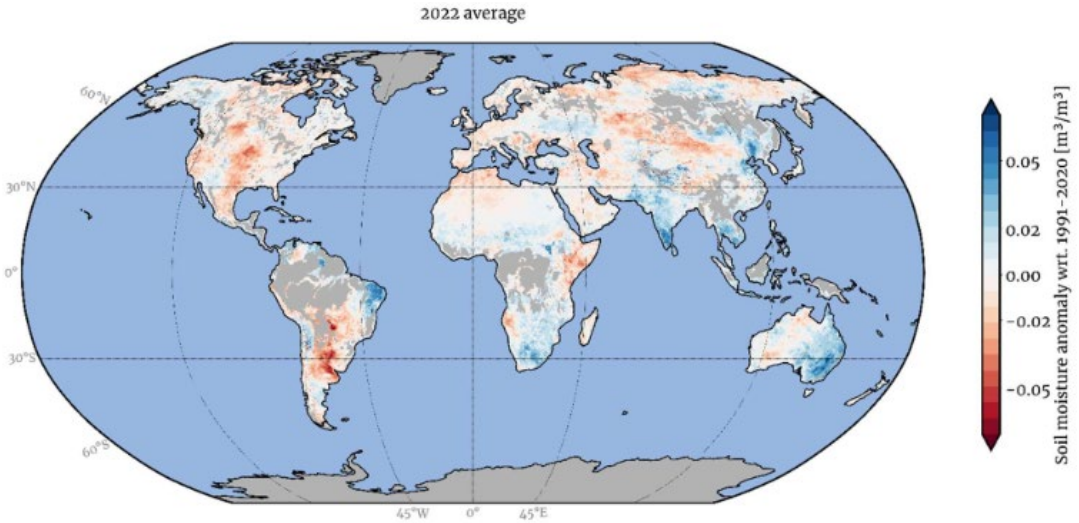

Figure 6: Mean Soil Moisture anomaly for 2022, with respect to the 1991-2020 baseline for the ESA CCI SM v08.1 COMBINED product, extracted from van der Schalie et al. (2023).

2.5. CCI Greenhouse Gasses

The Greenhouse Gasses (GHG) datasets provide observations of atmospheric methane (CH_4) and carbon dioxide (CO_2) amounts obtained from observations collected by several current and historical satellite instruments. They consist of two types of products: column-averaged mixing ratios of CO_2 and CH_4, denoted X CO_2 and X CH_4, and mid-tropospheric CO_2 and CH_4 columns, based on input data from different sensors: SCIAMACHY, TANSO-FTS, TANSO-FTS-2 and IASI. As in the case of Land Cover CCI, the algorithms developed for the processing of these datasets within the CCI project were later transferred to C3S to be generated operationally; they correspond to the Climate Research Data Package 7 (CRDP7) (Buchwitz et al. 2024). Data is provided in monthly files with spatial resolution from 10 km in the case of Level 2 products, to 5-deg for the Level 3 gridded product, and covering a time series from 2003 to 2022.

Further research within CCI+ extended the time series with new algorithms that produced X CO_2 and X CH_4 based on TANSO-FTS-2 for the period Feb-2019 to Dec-2023 (Barr et al. 2024) and a new X CH_4 dataset (version 1.8) based on Sentinel-5 TROPOMI data for the period Nov-2017 to Oct-2023 (Schneising 2024). Figure 7 shows the 2019-2020 biennal mean of X CH_4 of this latest product.

The GHG datasets will be used within the project for model benchmarking/validation for ML and process-based models.

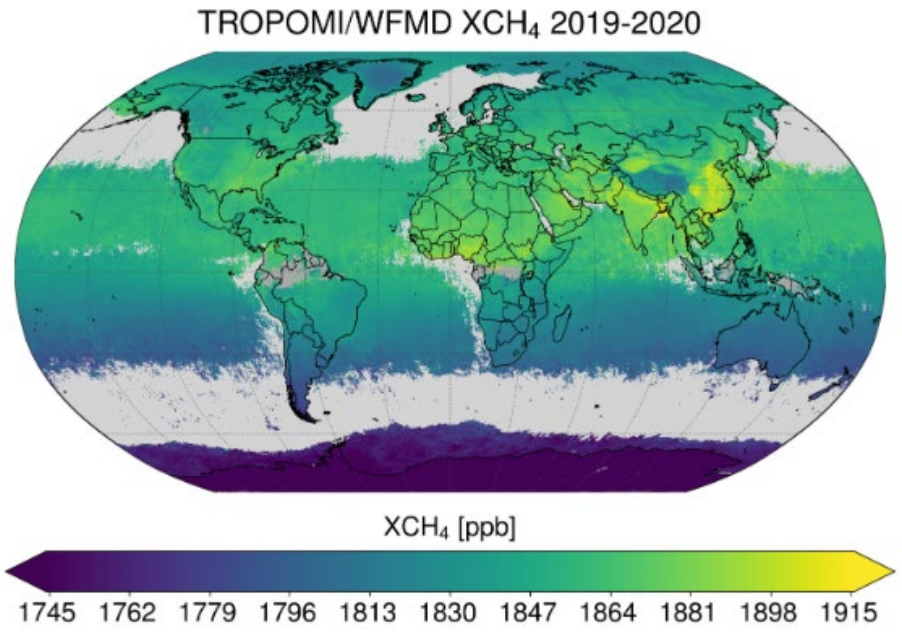

Figure 7: Biennal mean (2019-2020) of retrieved TROPOMI/WFMD v1.8 X CH_4, extracted from Schneising (2024).

2.6. CCI Aerosols

The Aerosol ECV provides monthly global datasets of total Aerosol Optical Depth (AOD) with information from several sensors: ATSR-2, AATSR, MERIS, POLDER, SLSTR, MODIS, VIIRS and OLCI at 1-degree spatial resolution from 1995 to 2023, based on a suite of different algorithms (Popp et al. 2024). These products have been transferred to C3S for their operational production, and can be downloaded from the Copernicus Datastore.

Figure 8 shows an example of the AOD for June 2018. These datasets will be considered for potential model benchmarking/validation (for the process-based model).

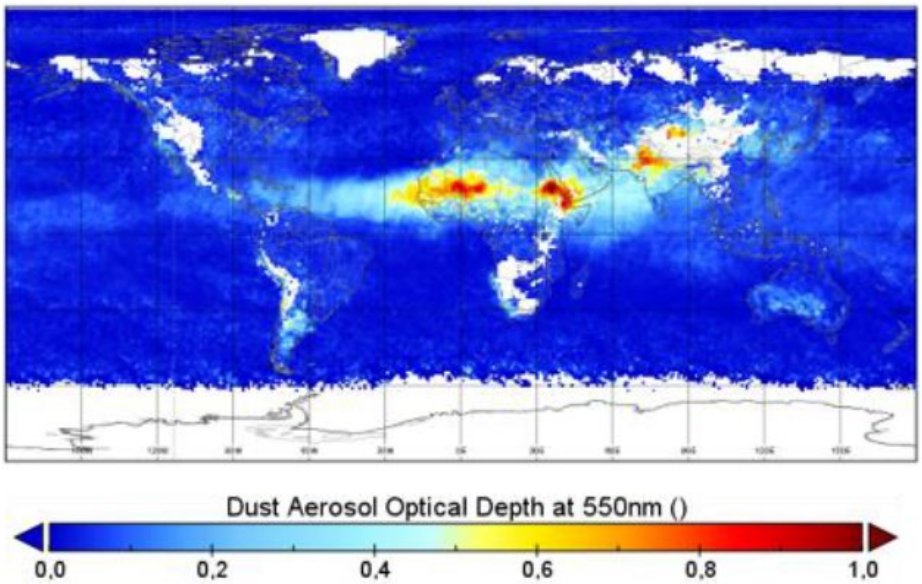

Figure 8: Dust AOD map for June 2018 from the LMD algorithm, extracted from Popp et al. (2024).

2.7. CCI Precursors

This ECV provides datasets of short-lived atmospheric trace gases, amongst which are the ones to be used in the project: nitrogen dioxide (NO_2) and carbon monoxide (CO). These datasets are based on different sensors including GOME, SCIAMACHY, GOME-2, OMI, TROPOMI, IASI and MOPITT. The CO products are available at 1-degree resolution for the period 2007-2023 in monthly files, while the NO_2 products are available, based on sensor data availability, between 1995 and 2023, in spatial resolutions between 0.2 and 1 degree, and as daily or monthly files (Boersma et al. 2024).

Figure 9 shows and example of a NO_2 map obtained for January 2019. These datasets will be used within the project for model benchmarking/validation for ML and process-based models.

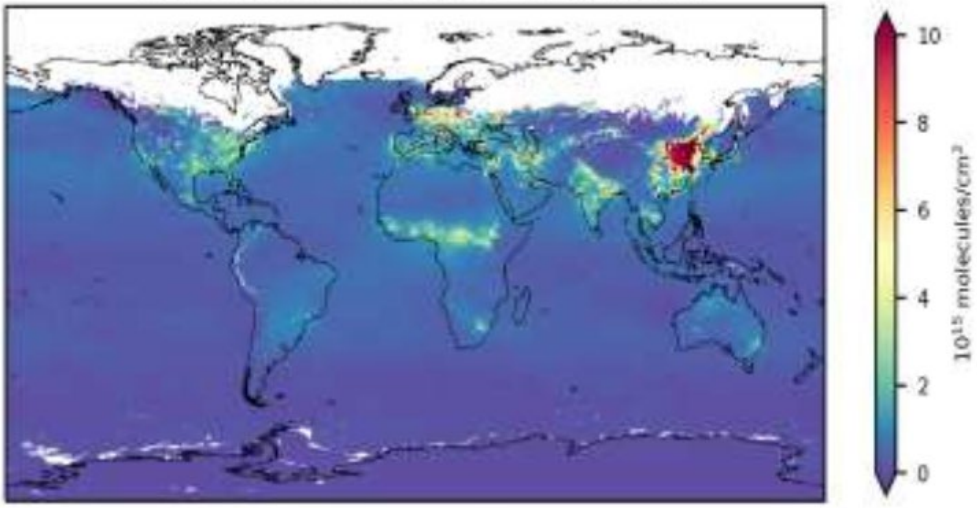

Figure 9: Mean tropospheric NO_2 column for January 2019 from TROPOMI data at 0.2-degree spatial resolution, extracted from Boersma et al. (2024).

2.8. CCI Lakes

The Lakes_cci product provides datasets related to the location and characteristics of inland water bodies with a global representative data coverage, based on lake area, availability of reference records, and priorities of the Copernicus programme (Calmettes et al. 2022). The current version is v2.1.0, and provides information of different parameters: Lake Water Level, Lake Water Extent, Lake Water-leaving Reflectance (LWLR), Lake Surface Water Temperature and Lake Ice Cover.

In particular, the LWLR, also known as water colour, is the measurement of the quantity of sunlight reaching the remote detector after interaction with the water column. From it, several optical- biogeochemical characteristics of the lake may be determined, including the concentration of phytoplankton pigment, particularly chlorophyll-a, the vertical transparency, the concentration of dissolved organic matter, and the total amount of suspended sediments. Figure 10 shows the inland water bodies included in the v2 dataset.

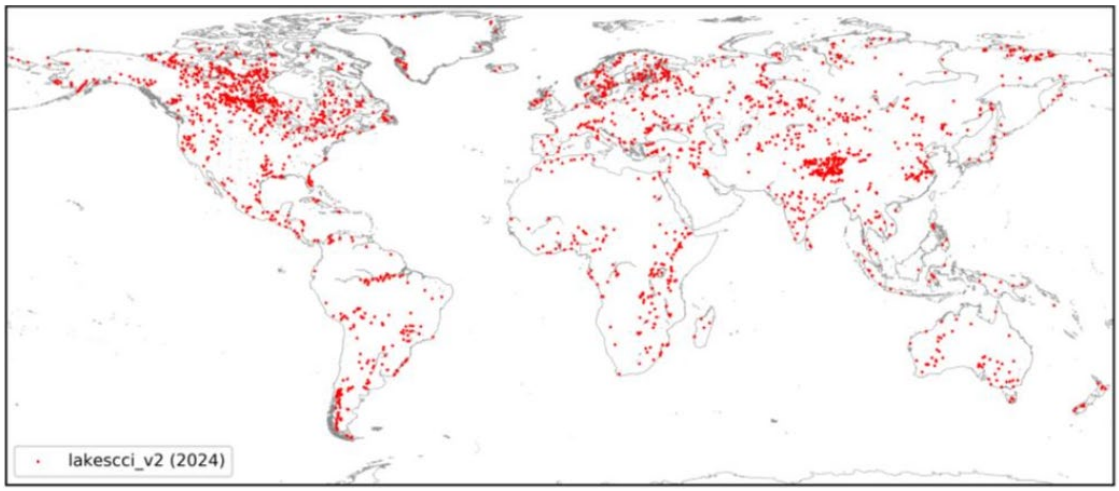

Figure 10: Inland water bodies included in Lakes_cci v2, from Simis et al. (2022).

Chlorophyll-a data from lakes has been previously analysed in relation to fire occurrence (Free et al. 2022, Giardino et al. 2023), and within XFires this analysis will be continued and improved as part of the tasks of the project. Complementary, it could be used as an input to the process-based models to increase the accuracy of burnable land areas.

2.9. CCI Ice Sheets (Greenland)

The Ice Sheets Greenland ECV produces data products of the following five parameters: surface elevation change (SEC), ice velocity, gravimetric mass balance, mass-flow rate ice discharge, and supraglacial lakes. Within the tasks of the project, the SEC parameter will be use to evaluate its change due to emissions from extreme fires.

The SEC parameter is obtained from radar altimetry missions (ERS-1, ERS-2, ENVISAT, CryoSat-2 and Sentinel-3), with a spatial resolution of 5 km in a polar stereographic grid, and for the period 1992-2019 in 5-yearly running means (Solgaard 2024).

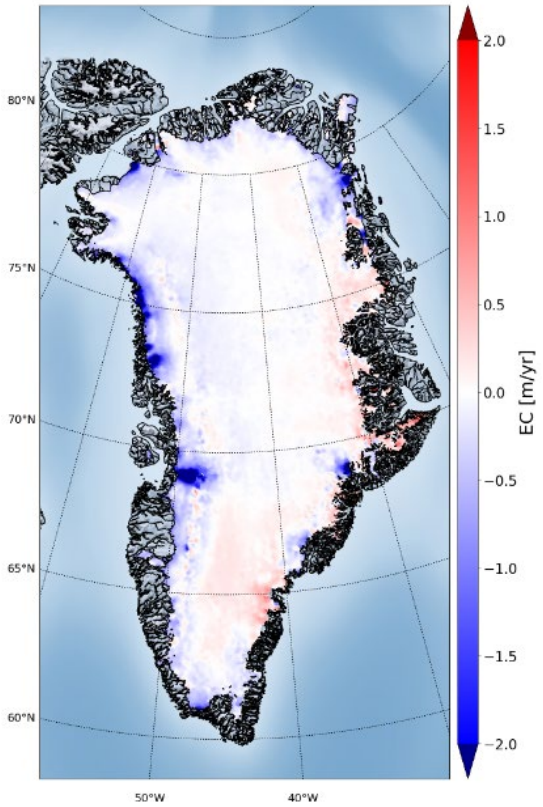

Figure 11: Surface elevation changes on a 5 km grid for the period 2012-2016, extracted from Solgaard (2024).

3. Other required datasets

Apart from the CCI datasets summarized in Section 2, another suite of products have been identified as needed to perform the activities of the project, and are cited in the following sub-sections.

3.1. GFED4s and GFED5

The Global Fire Emissions Database (GFED) databases provide maps of emissions from forest fires, based on burned area maps from the MOD64 Collection 6 product (Giglio et al. 2018), fuel biomass obtained from the CASA biosphere model, fuel consumption estimations, and emission factors to convert carbon losses to trace gas and aerosol emissions. GFED4s (van der Werf et al. 2017) has a time series from 1997 to 2023 (for the years 2017 to 2023 in beta version), at 0.25-degree spatial resolution. The newer version, GFED5, covers the period 1997-2020, and adds to the MOD64 burned area product a suite for finer resolution (from Landsat and Sentinel-2) existing datasets, including FireCCISFD11 (Roteta et al. 2019) and BARD (Burned Area Reference Database, Franquesa et al. 2020), which were developed as part of the FireCCI project.

The products are available as daily and monthly files, for more than 30 traces gasses and aerosol species. From those, CO_2 data will be used for fire model emissions validation and input for soil organic carbon (SOC) combustion estimation (for one method).

3.2. FINN v2.5

The Fire Inventory from National Center for Atmospheric Research (NCAR) version 2.5 (FINNv2.5) is a fire emissions inventory that provides publicly available emissions of trace gases and aerosols (Wiedinmyer et al. 2023). The information on burned areas is extracted from MODIS and VIIRS active fire detections, and is transformed to emissions using fuel consumption and emission factors applied to land cover maps from the MCD12Q1 version 6 product (Friedl et al. 2010) and VCF maps (see Section 3.7).

The dataset covers the period 2002 to 2023 in daily files at 0.1-degree spatial resolution. It includes more than 50 chemical species, from which CO_2 will be used for the same purposes as stated in Section 3.1.

3.3. CAMS

The Copernicus Atmospheric Monitoring Service (CAMS), managed by the European Centre for Medium-Range Weather Forecasts (ECMWF) (Inness et al., 2019) provides data products at two spatial resolutions. The reanalysis data have a spatial resolution of 0.75 degrees, and it is provided every 3 hours. CAMS also produces specific daily air quality analyses and forecasts for the European domain at significantly higher spatial resolution (0.1 degrees, approx. 10km) than is available from the global analyses and forecasts. The analysis combines model data with observations provided by the European Environment Agency (EEA) into a complete and consistent dataset using various data assimilation techniques depending upon the air-quality forecasting system used. In parallel, air quality forecasts are produced once a day for the next four days. Both the analysis and the forecast are available at hourly time steps and multiple height levels.

From this dataset, the project will use the $PM_{2.5}$ variable to analyse atmospheric conditions and the concentration of pollutants over study areas and their impacts on human health, due

to the high health risk associated with exposure to elevated concentrations (Chow et al., 2011).

3.4. SUOMI OMPS/VIIRS & AERONET AOD

The CCI AOD (Section 2.6) products will be used in addition with SUOMI VIIRS (Lee et al., 2024) and the Ozone Mapping and Profiler Suite -Nadir Mapper (OMPS-NM) (Seftor et al. 2014) to validate the performance of the Earth System Model. The OMPS-NM product is available since July 2011, while VIIRS is available since July 2014. Both products are operationally being produced in near real time.

Validation of model performance is difficult using standard satellite products. MODIS algorithms cannot retrieve the high AOD associated with smoke from extreme-fires nor can it determine the AOD when the aerosol co-exists in the column above, within or below clouds. However, the Suomi-OMPS Aerosol Index (AI) product does not suffer either such limitation. The AOD from the sun-photometer network will be correlated with the Suomi-OMPS AI derived from the OMPS-NM to derive an approximate AODOMPS. This is useful for assessing the model fidelity at high temporal resolution (i.e. daily) data owing as issues associated with cloud-screening are removed. Where there is no cloud, SUOMI VIIRS AOD will be used.

These datasets will be used to compare modelled AODs against observed AODs from AERONET (https://aeronet.gsfc.nasa.gov), AODOMPS and AODVIIRS.

3.5. FLUXNET

The FLUXNET2015 dataset provides ecosystem-scale data on CO_2, water, and energy exchange between the biosphere and the atmosphere, and other meteorological and biological measurements, from 212 sites around the globe (Pastorello et al. 2020). FLUXNET2015 includes derived-data products, such as gap-filled time series, ecosystem respiration and photosynthetic uptake estimates, estimation of uncertainties, and metadata about the measurements. The CO_2 fluxes include data on net ecosystem exchange, and its partition into ecosystem respiration and gross primary production components.

This dataset will be used as soil combustion model training and validation data.

3.6. ERA-5 and ERA-5 land

The fifth generation of European ReAnalysis (ERA5), is the latest ECMWF reanalysis for the global climate and weather for the past 8 decades. Data is available from 1940 onwards. ERA5 provides hourly estimates for a large number of atmospheric, ocean-wave and land-surface quantities. It has a horizontal resolution of 0.25 degrees, and it is provided with an hourly temporal resolution or monthly averaged data.

ERA5-Land is a reanalysis dataset providing a consistent view of the evolution of land variables over several decades at an enhanced resolution compared to ERA5. ERA5-Land (Muñoz-Sabater et al. 2021) has been produced by replaying the land component of the ERA5 climate reanalysis. This dataset is provided since January 2015 to present, in hourly time steps at a horizontal resolution of 0.1 degrees (from the native resolution of 9 km).

This dataset will be used as model input and for training data.

3.7. MOD44B

The MODIS/Terra Vegetation Continuous Fields (VCF) Yearly L3 Global 250m SIN grid product, designated as MOD44B, is a sub-pixel-level representation of surface vegetation cover estimates globally. It provides a gradation of three surface cover components: percent tree cover, percent non-tree cover, and percent bare, using monthly composites of Terra MODIS 250 and 500 meters Land Surface Reflectance data, including all seven bands, and Land Surface Temperature. It is produced globally at 250 m spatial resolution as yearly files, covering the period 2000 to 2022 (DiMiceli et al. 2021).

This dataset will be used as model input and for training data.

3.8. FORMS-H

The Forest Multiple Source (FORMS) is a height (FORMS-H), biomass and wood volume (FORMS-B/V) map in France at high resolution (10-30 m), based on Sentinel-1, Sentinel-2 and Global Ecosystem Dynamics Investigation (GEDI) data, and was developed using a deep learning approach (Schwartz et al. 2023). The maps are available for the year 2020.

The FORMS-H map at 10 m spatial resolution will be used as training data for quantifying biomass loss to extreme fires.

3.9. WoSIS

The World Soil Information Service (WoSIS) provides quality-assessed and standardised soil profile data to support digital soil mapping and environmental applications at broadscale levels (Batjes et al. 2020). It includes the following soil chemical properties: organic carbon, total carbon, total carbonate equivalent, total nitrogen, phosphorus (extractable P, total P and P retention), soil pH, cation exchange capacity and electrical conductivity. The latest dataset is comprised of 196 498 geo-referenced profiles originating from 173 countries (contributed by different data providers). They represent over 832 000 soil layers (or horizons) and over 5.8 million records.

This dataset will be used as input and output validation for ML and process-based soil combustion modelling.

3.10. North American boreal fire burn depth

This dataset was developed, first, with a new burned area algorithm across Alaska and Canada at 500 m spatial resolution that utilizes finer-scale 30 m Landsat imagery to account for land cover unsuitable for burning. Using this new burned-area product, statistical models to predict burn depth and carbon combustion were also developed (Potter et al. 2023). The dataset covers the period 2001 to 2019 in yearly files at 463 m spatial resolution.

The dataset is to be used to benchmark process-based, parameter-based and ML-derived estimates of direct soil carbon combustion by fire.

3.11. FireALT

The fire Active Layer Thickness (ALT) dataset gathers data contributions that include thaw depth measurements, site conditions, and fire event details with paired measurements at environmentally comparable burned and unburned sites (Talucci et al. 2024). It includes 52,466 thaw depth measurements from 18 contributors across North America and Russia. The

final dataset includes 47,952 ALT estimates (27,747 burned, 20,205 unburned) with 32 attributes. There are 193 unique paired burned/unburned sites spread across 12 ecozones that span Canada, Russia, and the United States. The data span fire events from 1900 to 2022.

This dataset will potentially be used to assess process-based modelling of soil thaw due to fire in high-latitude regions (legacy carbon impacts).

3.12. GLAKES

This Global Lakes (GLAKES) dataset mapped 3.4 million lakes on a global scale, including their explicit maximum extents and probability-weighted area changes over the past four decades (1984-2019). It is based on the Global Surface Water Occurrence dataset, which provides probability of water presence using 30 m spatial resolution Landsat data, after using deep learning algorithms for the disentanglement of lakes from rivers (Pi et al. 2022). The final dataset includes lakes with a size of 0.03 km^2 and larger.

This small lake addition supplements existing lake area data form Section 2.8 as input to process based models to increase accuracy of burnable land area.

3.13. WTD

The Water Table Depth (WTD) dataset presents global observations of water table depth compiled from government archives and literature from 1,603,781 well sites, and fills in data gaps and infer patterns and processes using a groundwater model forced by modern climate, terrain, and sea level (Fan et al. 2013). The simulated WTD has a resolution of 30 arc-seconds (approx. 1 km).

This dataset will be used as input to the process-based model.

3.14. Geomorpho90m

The Geomorpho90m global dataset comprises different geomorphometric features derived from the Multi-Error-Removed Improved Terrain (MERIT) Digital Elevation Model (DEM) (Amatulli et al. 2020). The fully-standardised 26 geomorphometric variables consist of layers that describe the (i) rate of change across the elevation gradient, using first and second derivatives, (ii) ruggedness, and (iii) geomorphological forms. The Geomorpho90m variables are available at 3 (~90 m) and 7.5 arc-second (~250 m) resolutions under the WGS84 geodetic datum, and 100 m spatial resolution under the Equi7 projection.

This dataset will be used as an input for process-based modelling of fragmentation fire interactions.

3.15. HYDE v3.2

The History Database of the Global Environment (HYDE) is an internally consistent combination of historical population estimates and allocation algorithms with time-dependent weighting maps for land use extracted from the CCI Land Cover product (see Section 2.2). Population is represented by maps of total, urban, rural population, population density and built-up area (Klein Goldewijk et al. 2017). The period covered is 10 000 before Common Era (BCE) to 2015 Common Era (CE). The population maps are available at 5 arc minutes spatial resolution. The time intervals vary, but for the period 2000-2015 the data is provided in yearly timesteps.

This global population density data will be used as an input to ML and process-based fire models.

3.16. GRIP

The Global Roads Inventory Project (GRIP) gathered, harmonized and integrated nearly 60 geospatial datasets on road infrastructure into a global roads dataset, comprising publicly available national and supra-national vector datasets from governments, research institutes, NGOs and crowdsource initiatives (Meijer et al. 2018). The resulting dataset covers 222 countries and includes over 21 million km of roads. Apart from the vector dataset, the product also includes gridded layers for road length (km of road per cell) and road density (meters of road per km^2 land area per cell) on a 5 × 5 arcminute resolution (approximately 8 × 8 km at the equator).

The gridded road density data will be used as input for process-based modelling of fragmentation fire interactions.

4. Summary of ECVs and their sources

The following table summarises the different datasets described in this document, including their sources and access points.

ECV	Source	Access Point
FireCCI51	ESA CCI – CEDA Catalogue	https://catalogue.ceda.ac.uk/uuid/3628cb2fdba443588155e15dee8e5352/
FRY2.0	ESA CCI	Currently available upon request to the FireCCI project team
CCI Biomass	ESA CCI – CEDA Catalogue	https://catalogue.ceda.ac.uk/uuid/bf535053562141c6bb7ad831f5998d77/
CCI Land Cover	ESA CCI – C3S	https://cds.climate.copernicus.eu/datasets/satellite-land-cover
CCI Land Surface Temperature	ESA CCI – CEDA Catalogue	https://data.ceda.ac.uk/neodc/esacci/land_surface_temperature/data
CCI Soil Moisture	ESA CCI – CEDA Catalogue	https://catalogue.ceda.ac.uk/uuid/b0f5fc3a10cf4806ab57326edd8daf65/
CCI Greenhouse Gasses	ESA CCI – CEDA Catalogue	https://data.ceda.ac.uk/neodc/esacci/ghg/data
CCI Aerosols	ESA CCI – C3S	https://cds.climate.copernicus.eu/datasets/satellite-aerosol-properties
CCI Precursors	ESA CCI	Currently available upon request to the CCI Precursors project team
CCI Lakes	ESA CCI – CEDA Catalogue	https://catalogue.ceda.ac.uk/uuid/7fc9df8070d34cacab8092e45ef276f1/

ECV	Source	Access Point
CCI Ice Sheets (Greenland)	ESA CCI – CEDA Catalogue	https://data.ceda.ac.uk/neodc/esacci/ice_sheets_greenland/data/greenland_surface_elevation_change
GFED4s	Global Fire Emissions Database	https://www.geo.vu.nl/~gwerf/GFED/GFED4/
GFED5	Global Fire Emissions Database	https://surfdrive.surf.nl/files/index.php/s/VPMEYinPeHtWVxn https://zenodo.org/records/7668424
FINN v2.5	National Center for Atmospheric Research	https://rda.ucar.edu/datasets/d312009/
CAMS	Copernicus Atmospheric Monitoring Service	https://ads.atmosphere.copernicus.eu/datasets/cams-europe-air-quality-forecasts-optimised-at-observation-sites
SUOMI OMPS AOD	NASA Earth Data	https://www.earthdata.nasa.gov/data/instruments/omps/near-real-time-data https://ozoneaq.gsfc.nasa.gov/data/aerosols/#
SUOMI VIIRS AOD	NOAA - EUMETSAT	https://user.eumetsat.int/catalogue/EO:EUM:DAT:0095/access
AERONET AOD	AERONET	https://aeronet.gsfc.nasa.gov/new_web/aerosols.html
FLUXNET	FLUXNET Network	https://fluxnet.org/data/fluxnet2015-dataset/
ERA-5	ECMWF - C3S	https://cds.climate.copernicus.eu/datasets/reanalysis-era5-single-levels
ERA-5 Land	ECMWF - C3S	https://cds.climate.copernicus.eu/datasets/derived-era5-land-daily-statistics
MOD44B	NASA – Earth Data	https://lpdaac.usgs.gov/products/mod44bv061/ https://e4ftl01.cr.usgs.gov/MOLT/MOD44B.061/
FORMS-H	Schwartz et al. (2023)	https://zenodo.org/records/7840108
WoSIS	ISRIC – World Soil Information	https://data.isric.org/geonetwork/srv/eng/catalog.search#/search?resultType=details&sortBy=relevance&any=wosis_latest&from=1&to=20
North American boreal fire burn depth	Potter et al. (2023)	https://daac.ornl.gov/cgi-bin/dsviewer.pl?ds_id=2063
FireALT	Talucci et al. (2024)	https://doi.org/10.18739/A2W950Q33

ECV	Source	Access Point
GLAKES	Pi et al. (2022)	https://zenodo.org/records/7016548
WTD	Fan et al. (2013)	Upon request to authors (website no longer online)
Geomorpho90m	Amatulli et al. (2020)	https://doi.pangaea.de/10.1594/PANGAEA.899135
HYDE v3.2	Klein Goldewijk et al. (2017)	https://geo.public.data.uu.nl/vault-hyde-data/HYDE%203.2[1648738557]
GRIP	GloBio	https://www.globio.info/download-grip-dataset

5. References

Alonso-González, E., Fernández-García, V. (2021) MOSEV: a global burn severity database from MODIS (2000–2020). Earth System Science Data, 13, 1925–1938 https://doi.org/10.5194/essd-13-1925-2021.

Amatulli, G., McInerney, D. et al (2020) Geomorpho90m, empirical evaluation and accuracy assessment of global high-resolution geomorphometric layers. Scientific Data 7, 162. https://doi.org/10.1038/s41597-020-0479-6

Barr, A.G., Borsdorff, T. et al (2024) Product User Guide (PUG) XCO2 GOSAT-2 SRON Full-Physics (CO2_GO2_SRFP) and XCH4 GOSAT-2 SRON Full-Physics (CH4_GO2_SRFP) version 5.0. https://climate.esa.int/media/documents/PUG_CRDP9_v2_GHG-CCI_CO2_CH4_GO2_SRFP_v2.0.3.pdf

Batjes, N. H., Ribeiro, E., and van Oostrum, A. (2020) Standardised soil profile data to support global mapping and modelling (WoSIS snapshot 2019), Earth System Science Data, 12, 299–320, https://doi.org/10.5194/essd-12-299-2020

Boersma, F., Clarisse, L. et al. (2024). Precursors_cci+ D4.2 Product User Guide, version 1.01. https://climate.esa.int/media/documents/Precursors_cci_D4.2_PUG_01_01.pdf

Buchwitz M., Reuter M. et al. (2024). Product User Guide and Specification (PUGS) – Main Document for Greenhouse Gas (GHG: CO2 & CH4) data set CDR7 (01.2003-12.2022). http://wdc.dlr.de/C3S_312b_Lot2/Documentation/GHG/C3S2_312a_Lot2_PUGS_GHG_main_latest.pdf

Calmettes, B., Simis, S. et al. (2022) CCI Lakes Product User Guide (PUG) v2.1. https://climate.esa.int/media/documents/CCI-LAKES-0029-PUG_v2.1.pdf

Carrea, L.; Crétaux, J.-F. et al. (2024): ESA Lakes Climate Change Initiative (Lakes_cci): Lake products, Version 2.1. NERC EDS Centre for Environmental Data Analysis, *04 April 2024*. https://dx.doi.org/10.5285/7fc9df8070d34cacab8092e45ef276f1

Chen, W., Campagnolo, M.L. et al. FRYv2.0: a global database of fire patch traits merging global spaceborne fire information (in revision).

Chow, J.C., Watson, J.G. et al. (2011) PM2.5 source profiles for black and organic carbon emission inventories. Atmospheric Environment 45(31), 5407–5414. https://doi.org/10.1016/j.atmosenv.2011.07.011

Defourny P., Lamarche C. et al. (2024) Product User Guide and Specification – CDR and ICDR Sentinel-3 Land Cover (v2.1.1), https://dast.copernicus-climate.eu/documents/satellite-land-cover/WP2-FDDP-LC-2021-2022-SENTINEL3-300m-v2.1.1_PUGS_v1.1_final.pdf

DiMiceli, C., Townshend, J. et al. (2021) Evolution of the representation of global vegetation by vegetation continuous fields. Remote Sensing of Environment 254, 112271. https://doi.org/10.1016/j.rse.2020.112271

ESA. Land Cover CCI Product User Guide Version 2. Tech. Rep. (2017). Available at: http://maps.elie.ucl.ac.be/CCI/viewer/download/ESACCI-LC-Ph2-PUGv2_2.0.pdf.

Fan, Y., Li, H. and Miguez-Camacho, G. (2013). Global patterns of Groundwater Table Depth. Science 339 (6122), 940-943. https://doi.org/10.1126/science.1229881

Franquesa, M., Vanderhoof, M. K. et al. (2020) Development of a standard database of reference sites for validating global burned area products, Earth System Science Data 12, 3229–3246. https://doi.org/10.5194/essd-12-3229-2020

Free G., Stroppiana D. et al. (2022) Effects of Wildfires on Lakes. Study Report: State of the art and selection of study areas. https://climate.esa.int/media/documents/CCI-LAKES-0076-CCN_EffectsonWildfiresOnLakes_D1-v1.1.pdf

Friedl, M. A., Sulla-Menashe, D. et al. (2010). MODIS Collection 5 global land cover: Algorithm refinements and characterization of new datasets. Remote Sensing of Environment, 114, 168-182. https://doi.org/10.1016/j.rse.2009.08.016

Ghent, D., Dodd, E. et al. (2023) CCI Land Surface Temperature Algorithm Theoretical Basis Document v4.0. https://admin.climate.esa.int/media/documents/LST-CCI-D2.2-ATBD_-_i4r0_-_Algorithm_Theoretical_Basis_Document.pdf

Ghent, D., Ermida S. et al. (2021) CCI Land Surface Temperature User Guide v2.0. https://admin.climate.esa.int/media/documents/LST-CCI-D4.3-PUG_-_i2r0_-_Product_User_Guide.pdf

Giardino C., Pinardi, M. et al. (2023) Effects of Wildfires on Lakes. Study Report: Regional and global impact of wildfires on lakes. https://climate.esa.int/media/documents/CCI-LAKES-0080_CCN4_EffectsonWildfiresOnLakes_D3.pdf

Giglio, L., Boschetti, L. et al. (2018) The Collection 6 MODIS burned area mapping algorithm and product. Remote Sensing of Environment 217, 72-85. https://doi.org/10.1016/j.rse.2018.08.005

Giglio, L., Schroeder, W. et al. (2016) The collection 6 MODIS active fire detection algorithm and fire products. Remote Sensing of Environment, 178, 31-41. https://doi.org/10.1016/j.rse.2016.02.054

Inness, A., Ades, M. et al. (2019) The CAMS reanalysis of atmospheric composition. Atmospheric Chemistry and Physics 19(6), 3515–3556. https://doi.org/10.5194/acp-19-3515-2019

Klein Goldewijk, K., Beusen A. et al. (2017) Anthropogenic land use estimates for the Holocene – HYDE 3.2, Earth System Science Data 9, 927–953. https://doi.org/10.5194/essd-9-927-2017

Laurent, P., Mouillot, F. et al. (2019) Varying relationships between fire radiative power and fire size at a global scale. Biogeosciences, 16(2), 275–288. https://doi.org/10.5194/bg-16-275-2019

Lee, J., Hsu, N. C. et al. (2024). VIIRS Version 2 Deep Blue aerosol products. Journal of Geophysical Research: Atmospheres, 129, e2023JD040082. https://doi.org/10.1029/2023JD040082

Lizundia-Loiola J., Pettinari M. L. et al. (2018). "ESA CCI ECV Fire Disturbance: Algorithm Theoretical Basis Document-MODIS, version 2.0." Fire_cci_D2.1.3_ATBD-MODIS_v2.0. https://climate.esa.int/media/documents/Fire_cci_D2.1.3_ATBD-MODIS_v2.0.pdf

Lizundia-Loiola, J., Otón, G. et al. (2020) A spatio-temporal active-fire clustering approach for global burned area mapping at 250 m from MODIS data. Remote Sensing of Environment 236: 111493, https://doi.org/10.1016/ j.rse.2019.111493

Meijer, J. R., Huijbregts, M. A. J. et al. (2018) Global patterns of current and future road infrastructure. Environmental Research Letters 13, 064006. https://doi.org/10.1088/1748-9326/aabd42

Muñoz-Sabater, J., Dutra, E. et al. (2021). ERA5-Land: a state-of-the-art global reanalysis dataset for land applications. Earth System Science Data 13 (9), 4349, 4383. https://doi.org/10.5194/essd-13-4349-2021

Pastorello, G., Trotta, C. et al. (2020) The FLUXNET2015 dataset and the ONEFlux processing pipeline for eddy covariance data. Scientific Data 7, 225. https://doi.org/10.1038/s41597-020-0534-3

Pi, X., Luo, Q. et al. (2022) Mapping global lake dynamics reveals the emerging roles of small lakes. Nature Communications 13, 5777. https://doi.org/10.1038/s41467-022-33239-3

Popp, T., Goussev, O. et al. (2024) Product User Guide and Specification – Aerosol Products v2.0. https://dast.copernicus-climate.eu/documents/satellite-aerosol-properties/C3S2_312a_Lot2_FDDP-AER/C3S2_312a_Lot2_D-WP2-FDDP-AER_202311_PUGS_AER_v2.0_final2.pdf

Potter, S., Cooperdock, S. et al. (2023). Burned area and carbon emissions across northwestern boreal North America from 2001–2019, Biogeosciences, 20, 2785–2804, https://doi.org/10.5194/bg-20-2785-2023

Roteta, E., Bastarrika, A., et al. (2019) Development of a Sentinel-2 burned area algorithm: Generation of a small fire database for sub-Saharan Africa. Remote Sensing of Environment 222, 1–17, https://doi.org/10.1016/j.rse.2018.12.011

Santoro, M., Cartus, O., et al. (2024). CCI Biomass Product User Guide v5. https://climate.esa.int/media/documents/D4.3_CCI_PUG_V5.0_20240617.pdf

Schneising O. (2024) Product User Guide (PUG) TROPOMI WFM-DOAS (TROPOMI/WFMD) XCH4 v1.8. https://climate.esa.int/media/documents/PUG_CRDP9_v2_GHG-CCI_CH4_S5P_WFMD_v1.8.pdf

Schwartz, M., Ciais, P. et al. (2023). FORMS: Forest Multiple Source height, wood volume, and biomass maps in France at 10 to 30 m resolution based on Sentinel-1, Sentinel-2, and Global Ecosystem Dynamics Investigation (GEDI) data with a deep learning approach. Earth System Science Data 15 (11), 4927-4945. https://doi.org/10.5194/essd-15-4927-2023

Seftor, C.J. Jaross, G. et al. (2014) Postlaunch performance of the Suomi National Polar-orbiting Partnership Ozone Mapping and Profiler Suite (OMPS) nadir sensors. JGR Atmospheres 119 (7). https://doi.org/10.1002/2013JD020472

Solgaard, A. (2024). Greenland_Ice_Sheet_cci+ Product User Guide for CCI+ Phase 2 version 3.1. https://climate.esa.int/media/documents/DTU-ESA-GISCCI-PUG-001_v3.1.pdf

Talucci, A., Loranty, M. M. et al. (2024) Permafrost-wildfire interactions: Active layer thickness estimates for paired burned and unburned sites in northern high-latitudes, Earth Syst. Sci. Data Discuss. [preprint], https://doi.org/10.5194/essd-2024-526, in review.

van der Schalie, R., Preimesberger W. et al. (2023) Soil Moisture Product User Guide supporting Product Version v08.1 https://zenodo.org/records/8320914

van der Werf, G.R., Randerson, J.T. et al. (2017) Global fire emissions estimates during 1997-2016. Earth System Science Data 9, 697-720. https://doi.org/10.5194/essd-9-697-2017

Wiedinmyer, C., Kimura, Y. et al. (2023) The Fire Inventory from NCAR version 2.5: an updated global fire emissions model for climate and chemistry applications, Geoscientific Model Development 16, 3873–3891, https://doi.org/10.5194/gmd-16-3873-2023

Annex 1 Acronyms and abbreviations

AGB	Above Ground Biomass
AI	Aerosol Index
ALT	Active Layer Thickness
AOD	Aerosol Optical Depth
AODOMPS	Aerosol Optical Depth from OMPS
AODVIIRS	Aerosol Optical Depth from VIIRS
BA	Burned Area
C3S	Copernicus Climate Change Service
CAMS	Copernicus Atmospheric Monitoring Service
CASA	Carnegie-Ames-Stanford Approach
CCI	Climate Change Initiative
CH_4	Methane
CO	Carbon Monoxide
CO_2	Carbon Dioxide
CRDP	Climate Research Data Package
DEM	Digital Elevation Model
ECMWF	European Centre for Medium-Range Weather Forecasts
ECV	Essential Climate Variable
EEA	European Environment Agency
ERA5	Fifth generation of European ReAnalysis
ESA	European Space Agency
ESRI	Environmental Systems Research Institute
FORMS	Forest Multiple Source
FRP	Fire Radiative Power
FRY	FiRe patch morphologY
GEDI	Global Ecosystem Dynamics Investigation
GFED	Global Fire Emissions Database
GHG	Greenhouse Gasses
GLAKES	Global Lakes
GOME	Global Ozone Monitoring Experiment
HYDE	History Database of the Global Environment
IASI	Infrared Atmospheric Sounding Interferometer
LCCS	Land Cover Classification System
LST	Land Surface Temperature
LWLR	Lake Water-leaving Reflectance
MERIS	Medium Resolution Imaging Spectrometer
MERIT	Multi-Error-Removed Improved Terrain
ML	Machine learning
MODIS	Moderate Resolution Imaging Spectroradiometer
MOPITT	Measurement of Pollution in the Troposphere
NCAR	National Center for Atmospheric Research
NIR	Near InfraRed
NO_2	Nitrogen Dioxide
NRT	Near Real Time

OLCI	Ocean and Land Colour Instrument
OMI	Ozone Monitoring Instrument
OMPS	Ozone Mapping and Profiler Suite
$PM_{2.5}$	Particulate Matter of 2.5 microns
POLDER	POLarization and Directionality of the Earth's Reflectances
SCIAMACHY	SCanning Imaging Absorption spectrometer for Atmospheric ChartographY
SEC	Surface Elevation Change
SLSTR	Sea and Land Surface Temperature Radiometer
SM	Soil Moisture
SOC	Soil Organic Carbon
TANSO-FTS	Thermal And Near infrared Sensor for carbon Observation - Fourier Transform Spectrometer
TROPOMI	TROPOsferic Monitoring Instrument
VCF	Vegetation Continuous Field
VIIRS	Visible Infrared Imaging Radiometer Suite
WFMD	Weighting Function Modified Differential Optical Absorption Spectroscopy.
WTD	Water Table Depth